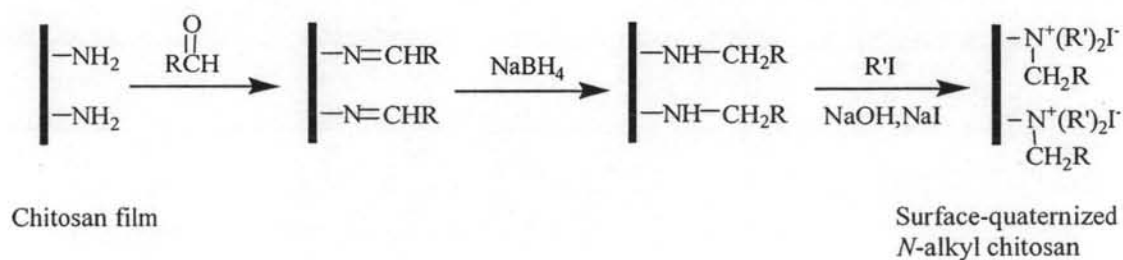


CHAPTER IV

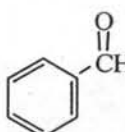
RESULTS AND DISCUSSION

This chapter is divided into 2 sections. The first section is dedicated to the preparation of two series of surface-quaternized *N*-alkyl chitosan by reductive *N*-alkylation using selected aldehydes followed by quaternization using selected alkyl iodides (See Table 4.1). The second section involves the determination of antibacterial activities of the quaternized *N*-alkyl chitosan having different alkyl group and extent of quaternization.



Scheme 4.1 Surface quaternization of chitosan film

Table 4.1 Aldehydes and alkyl iodides used for surface quaternization

$\begin{array}{c} \text{O} \\ \parallel \\ \text{RCH} \end{array}$	R'I	Product
$\begin{array}{c} \text{O} \\ \parallel \\ \text{HCH} \end{array}$	$\text{CH}_3\text{CH}_2\text{I}$	$\begin{array}{c} \\ -\text{N}^+(\text{CH}_2\text{CH}_3)_2\text{I}^- \\ \\ \text{CH}_3 \end{array}$
	$\text{CH}_3\text{CH}_2\text{CH}_2\text{CH}_2\text{I}$	$\begin{array}{c} \\ -\text{N}^+(\text{CH}_2\text{CH}_2\text{CH}_2\text{CH}_3)_2\text{I}^- \\ \\ \text{CH}_3 \end{array}$
	$\text{CH}_3\text{CH}_2\text{CH}_2\text{CH}_2\text{CH}_2\text{CH}_2\text{CH}_2\text{CH}_2\text{I}$	$\begin{array}{c} \\ -\text{N}^+(\text{CH}_2\text{CH}_2\text{CH}_2\text{CH}_2\text{CH}_2\text{CH}_2\text{CH}_2\text{CH}_2\text{CH}_3)_2\text{I}^- \\ \\ \text{CH}_3 \end{array}$
$\begin{array}{c} \text{O} \\ \parallel \\ \text{CH}_3\text{CH} \end{array}$	CH_3I	$\begin{array}{c} \\ -\text{N}^+(\text{CH}_3)_2\text{I}^- \\ \\ \text{CH}_2\text{CH}_3 \end{array}$
$\begin{array}{c} \text{O} \\ \parallel \\ \text{CH}_3\text{CH}_2\text{CH} \end{array}$		$\begin{array}{c} \\ -\text{N}^+(\text{CH}_3)_2\text{I}^- \\ \\ \text{CH}_2\text{CH}_2\text{CH}_3 \end{array}$
$\begin{array}{c} \text{O} \\ \parallel \\ \text{CH}_3\text{CH}_2\text{CH}_2\text{CH} \end{array}$		$\begin{array}{c} \\ -\text{N}^+(\text{CH}_3)_2\text{I}^- \\ \\ \text{CH}_2\text{CH}_2\text{CH}_2\text{CH}_3 \end{array}$
		$\begin{array}{c} \\ -\text{N}^+(\text{CH}_3)_2\text{I}^- \\ \\ \text{CH}_2 \\ \\ \text{C}_6\text{H}_5 \end{array}$

4.1 Determination of % Degree of Deacetylation (%DD) of Chitosan

Percentage of substitution of the amino group of chitosan by charge functionality can be calculated from a number of amino groups available per chain of chitosan which is generally expressed as a degree of deacetylation (%DD). %DD is defined as the percentage of glucosamine units in the chitosan chain and can be determined by NMR analysis. According to ^1H NMR spectrum of an original chitosan film shown in Figure 4.1, there is a broad signal at 3.3-3.7 ppm, assigned to $\text{H}_2, \text{H}_3, \text{H}_4, \text{H}_5$ and H_6 , and a signal between 4.5 and 5.0 ppm, assigned to H_1 protons. The signal for H_2 is at 2.89 ppm. Integrations of methyl protons from *acetamides* ($-\text{CH}_3$ of

GlcNAc, δ 1.71 ppm) and proton ($-\underline{\text{C}}\text{H}\text{NH}_2$ of GlcN, δ 2.89 ppm) are shown in Table 4.2.

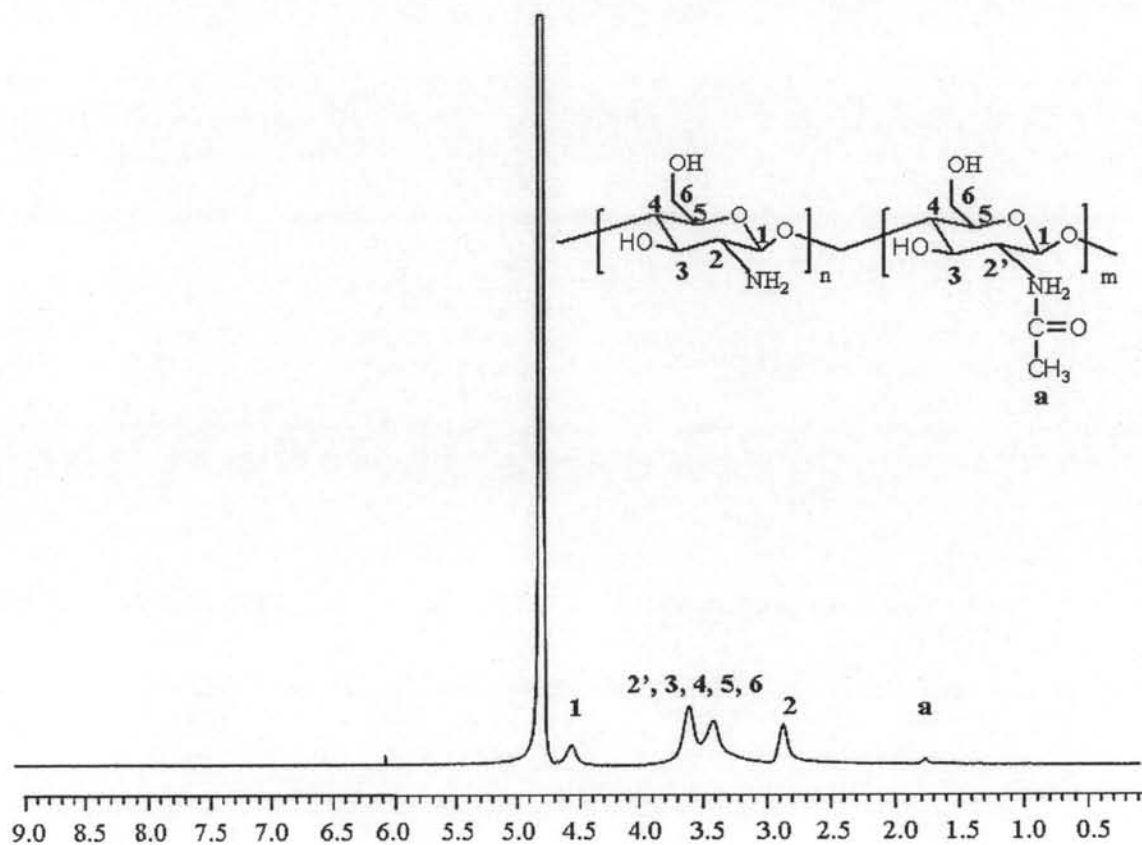


Figure 4.1 ^1H NMR spectrum of chitosan from Seafresh Chitosan (Lab) Co., Ltd. (solvent: 1% CF_3COOH in D_2O , 25°C).

Table 4.2 Information from ^1H NMR spectrum of chitosan used in this study

	δ (ppm)	Integration	Relative Amount of units
$-\underline{\text{C}}\text{H}\text{NH}_2$ of GlcN	2.89	16.7	16.7/1
$-\underline{\text{C}}\text{H}_3$ of GlcNAc	1.78	4.8	4.8/3

Considering the total repeating units in chitosan as 100%, %DD of 91 % was calculated based on the data in Table 4.2 using the following equation.

$$\%DD = \frac{\text{Amount of GlcN unit in chitosan}}{\text{The total amount of GlcN and GlcNAc units in chitosan}} \times 100$$

$$= \frac{(16.7/1) \times 100\%}{(4.8/3) + (16.7/1)} = 91\%$$

4.2 Preparation of *N*-alkyl Chitosan Films

Contact angle measurement, one of the most convenient surface-sensitive techniques, was first used as a primary tool to monitor the extent of both *N*-alkylation and quaternization as a function of reaction time and reagent concentration to obtain optimized condition. Figure 4.2 displays the water contact angles of the chitosan films after reductive *N*-alkylation as a function of aldehyde concentration. Obviously, the greater extent of reaction made the chitosan more hydrophilic using formaldehyde and acetaldehyde. This can be explained as a result of the H-bonding between the amino groups and the crystallinity of chitosan being destroyed after the reaction. The trend was reversed, however, in the case of larger aldehydes: propionaldehyde, butyraldehyde, benzaldehyde. The longer and larger alkyl groups from these aldehydes intrinsically introduced additional hydrophobicity to the chitosan films and masking the influence from the reduction of crystallinity.

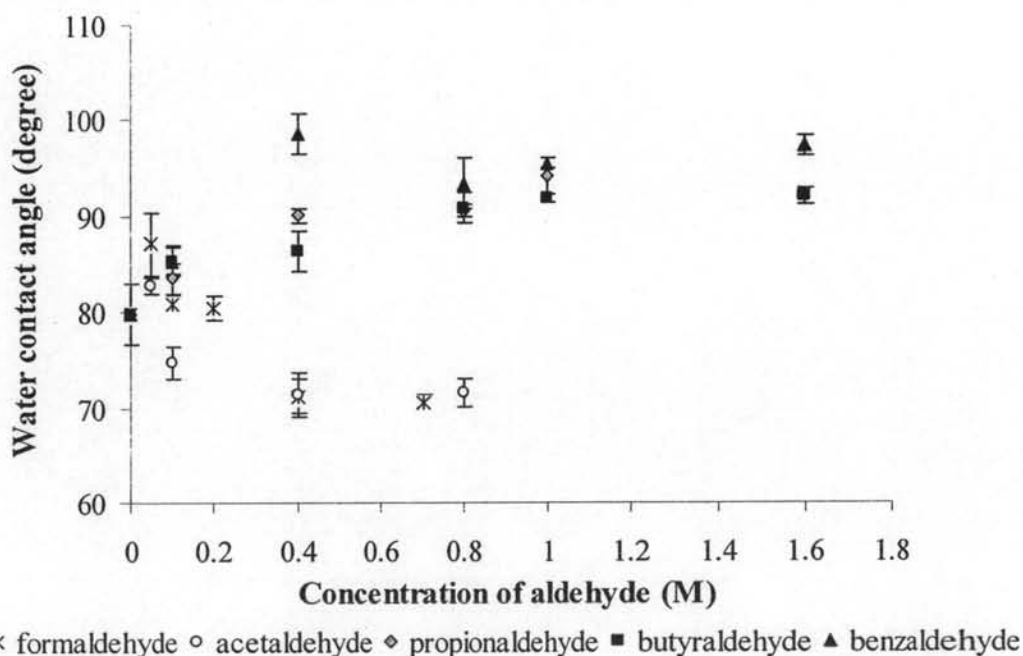
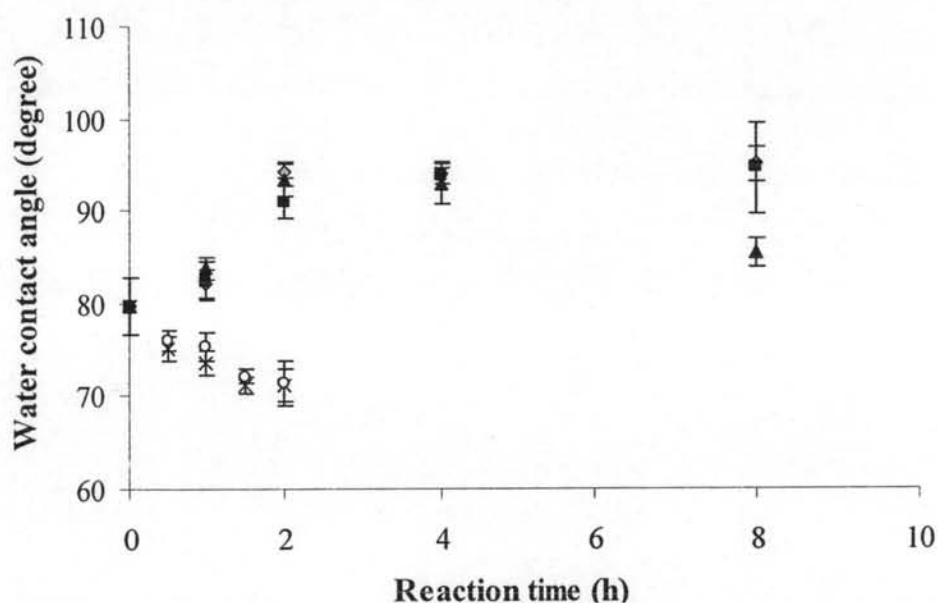


Figure 4.2 Water contact angle of chitosan film after reductive *N*-alkylation for 2h as a function of aldehyde concentration

Effect of reaction time in the step of imine formation between the amino groups of chitosan and aldehyde prior to the addition of NaBH_4 on the extent of reaction was also investigated. The results plotted in Figure 4.3 suggested that 4h was enough to attain the maximum extent of surface modification in the case of propionaldehyde, butyraldehyde, benzaldehyde. It was found that the chitosan films became quite brittle if they were exposed to the solution of formaldehyde and acetaldehyde beyond 1.5 h. It was believed that the small aldehydes can efficiently penetrate quite deeply inside the film and thus damaged their original mechanical integrity. For this reason, 1.5 h was used for reductive *N*-alkylation using formaldehyde and acetaldehyde. The optimized condition for the step of reductive *N*-alkylation is listed in Table 4.3.



* formaldehyde o acetaldehyde ◇ propionaldehyde ■ butyraldehyde ▲ benzaldehyde

Figure 4.3 Water contact angle of chitosan film after reductive *N*-alkylation using the optimized concentration of each aldehyde as a function of reaction time

Table 4.3 Optimized conditions for reductive *N*-alkylation of chitosan films

Aldehyde	Concentration (M)	Time (h)
Formaldehyde	0.4	1.5
Acetaldehyde	0.4	1.5
Propionaldehyde	1.0	4
Butyraldehyde	1.0	4
Benzaldehyde	1.0	4

4.3 Preparation of Quaternized *N*-alkyl Chitosan films

Using the optimized conditions for *N*-reductive alkylation, two series of quaternized *N*-alkyl chitosan films were prepared. The first series employed *N*-methyl chitosan films as substrates. Three different alkyl iodides which are ethyl iodide (EtI), butyl iodide (BuI) and octyl iodide (OcI) were used for quaternization. The quaternization of *N*-methyl chitosan film with EtI, BuI and OcI yielded *N*-methyl-*N,N*-diethyl chitosan (DEM) film, *N*-methyl-*N,N*-dibutyl chitosan (DBuM) film and *N*-methyl-*N,N*-dioctyl chitosan (DOM) film, respectively. As anticipated, the contact angles of *N*-methyl chitosan films were raised after the additional ethyl and butyl groups were introduced by quaternization. According to Figure 4.4, the optimized concentration of EtI and BuI for quaternization was 2 M. The unchanged contact angle of the *N*-methyl chitosan films after quaternization by OcI implied that OcI is a sterically hindered substrate so that the nucleophilic substitution by amino group of the *N*-methyl chitosan failed to occur. The results from Figure 4.5 suggested that 12 h was certainly enough to obtain the maximum quaternization for both EtI and BuI.

The second series of quaternized *N*-alkyl chitosan films were prepared using 5 different *N*-alkyl chitosan films as substrates and methyl iodide (MeI) as the reagent for quaternization. The quaternization of *N*-ethyl chitosan film, *N*-propyl chitosan film, *N*-butyl chitosan film and *N*-benzyl chitosan film yielded *N*-ethyl-*N,N*-dimethyl chitosan (DME) film, *N*-propyl-*N,N*-dimethyl chitosan (DMP) film, *N*-butyl-*N,N*-dimethyl chitosan (DMBu) film and *N*-benzyl-*N,N*-dimethyl chitosan (DMBz) film, respectively. According to Figures 4.6-4.7, the surface of all *N*-alkyl chitosan films

essentially became more hydrophilic after quaternization. Optimized quaternization conditions for all *N*-alkyl chitosan substrates are displayed in Table 4.4.

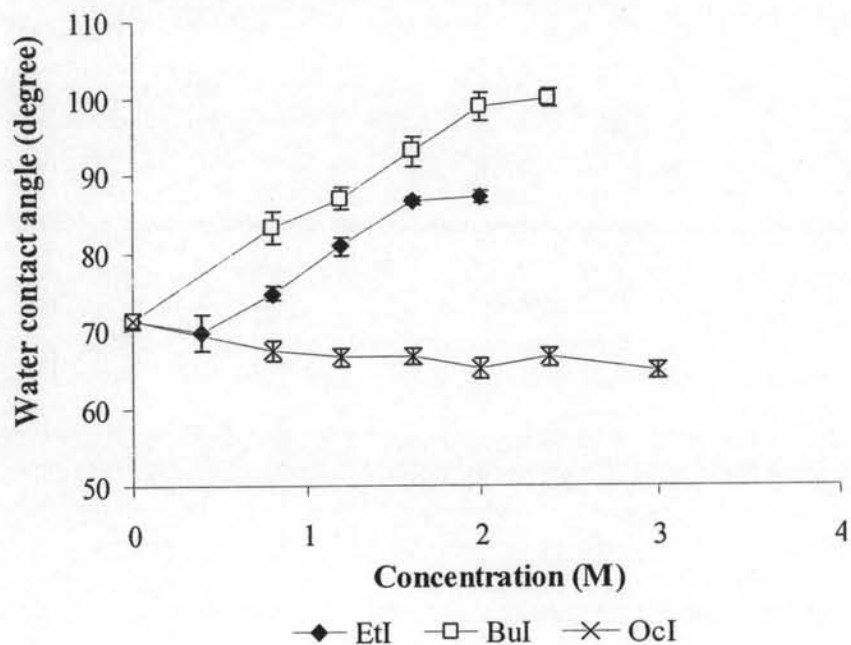


Figure 4.4 Water contact angle of *N*-methyl chitosan films after quaternization for 12 h as a function of alkyl iodide concentration

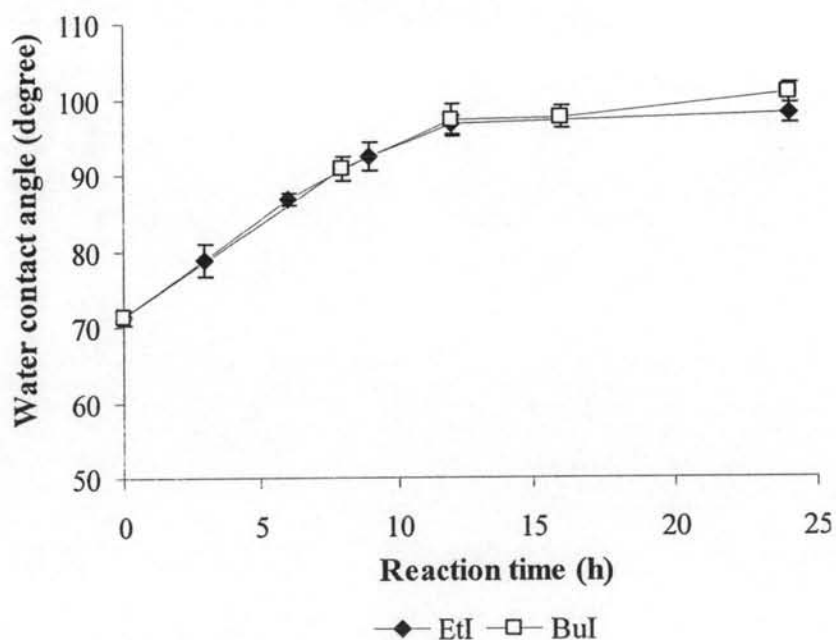


Figure 4.5 Water contact angle of *N*-methyl chitosan films after quaternization using the optimized concentration of each alkyl iodide as a function of reaction time

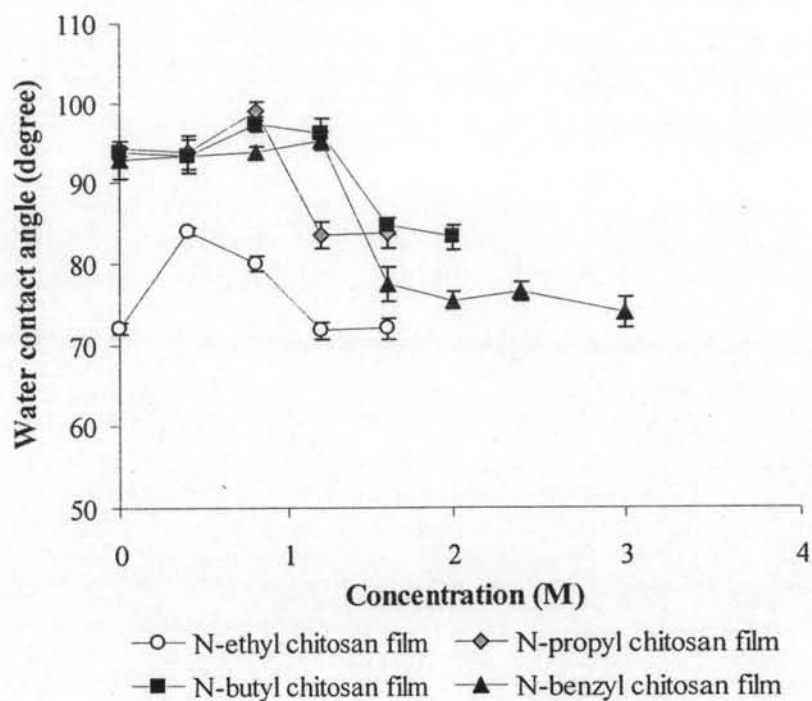


Figure 4.6 Water contact angle of *N*-alkyl chitosan films after quaternization for 12 h as a function of methyl iodide concentration

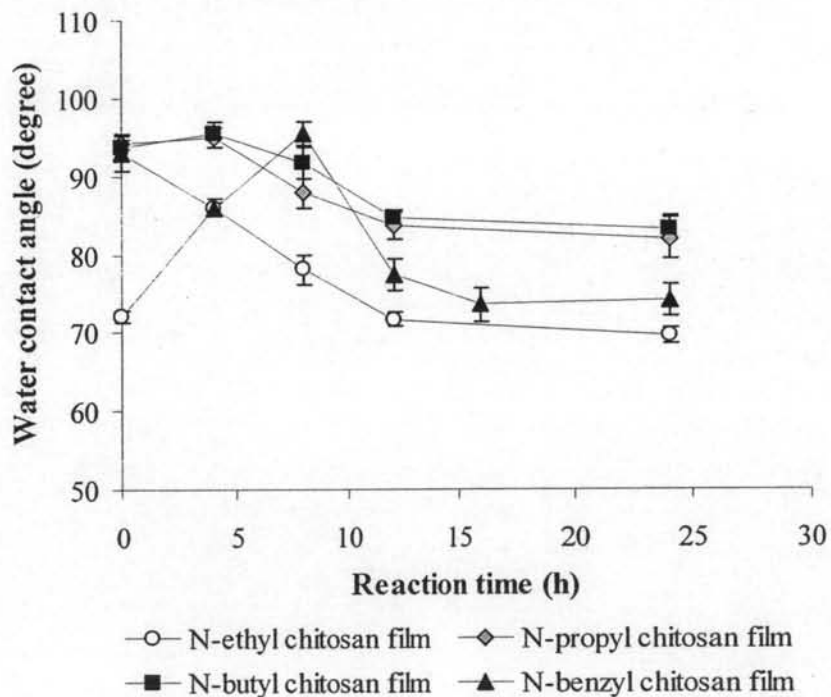


Figure 4.7 Water contact angle of *N*-alkyl chitosan films after quaternization using the optimized concentration of methyl iodide for each substrate as a function of reaction time

Table 4.4 Optimized conditions for quaternization of *N*-alkyl chitosan films with MeI

Substrate	MeI (M)	Time (h)
<i>N</i> -ethyl chitosan film	1.2	12
<i>N</i> -propyl chitosan film	1.2	12
<i>N</i> -butyl chitosan film	1.6	12
<i>N</i> -benzyl chitosan film	2.0	12

From ^1H NMR spectra of *N*-alkyl chitosan films after quaternization by MeI illustrated in Figure 4.8, the signal at 3.1 ppm was assigned to the methyl protons of the quaternary ammonium group while the signal at 2.8 ppm was assigned to the methyl protons of the disubstituted amino groups. In the case of DMBz film (Figure 4.8(e)), the signals of aromatic proton at 7.2 ppm evidently confirm the attachment of benzyl groups at the amino moieties of chitosan. In the cases of DME, DMP and DMBu films, no signal of ethyl, propyl and butyl protons which should have appeared at 0.80 ppm (methyl protons) and 1.11 ppm (methylene protons) were observed. These results suggested that the extent of benzyl substitution in the step of reductive alkylation using the optimized condition was greater than other alkyl groups presumably due to an electronic effect. Electron-withdrawing through resonance effect of the benzyl group makes a carbonyl carbon of benzaldehyde more reactive towards the nucleophilic attack of the amino group of chitosan.

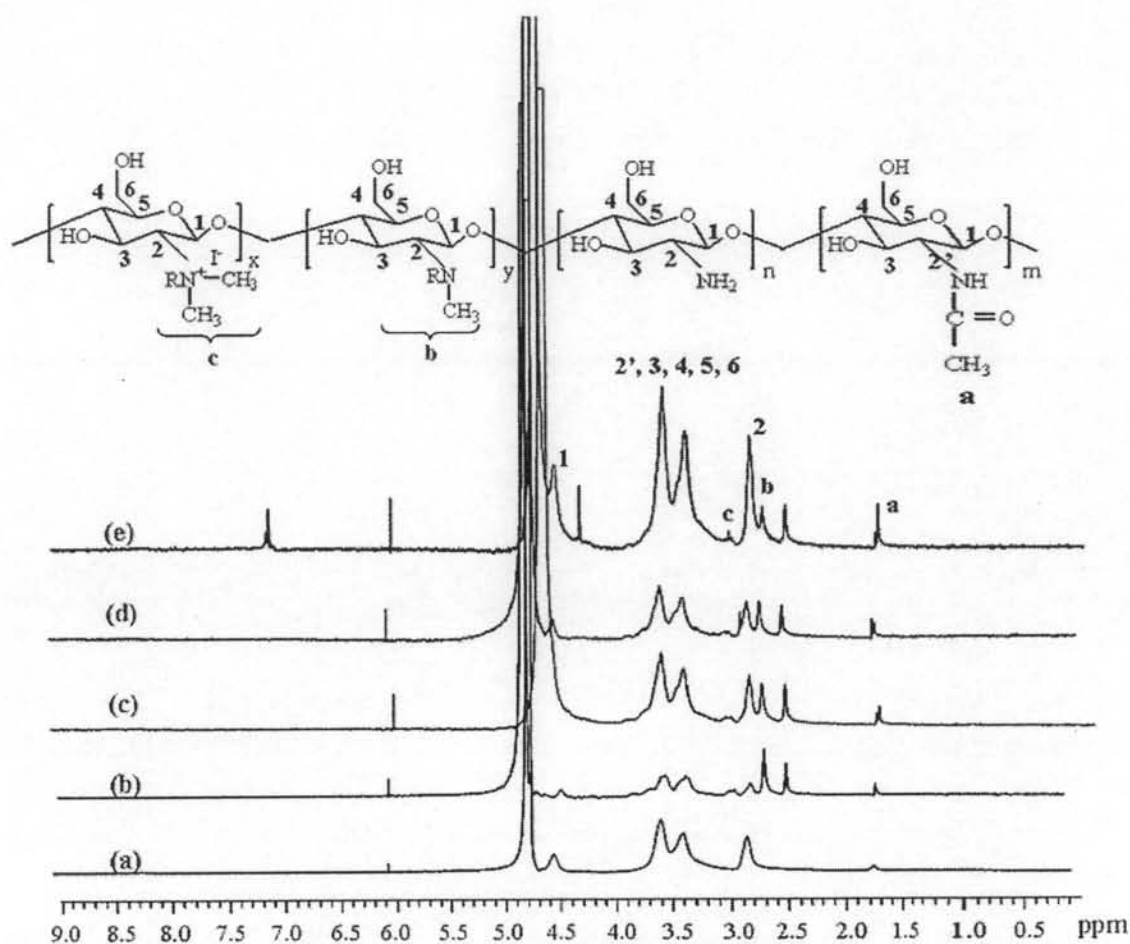


Figure 4.8 ^1H NMR spectra of (a) unmodified chitosan film, (b) DME film, (c) DMP film, (d) DMBu film and (e) DMBz film.

Evidences from the NMR analysis implied that the surface modification proceeded so deeply that the quaternization can be realized by a bulk technique like ^1H NMR. The degree of quaternization can be determined from the relative ratio between the integration of 6 protons from 2 methyl groups of quaternized *N*-alkyl chitosan and the peak integration of 5 protons of chitosan (δ 3.4-3.8 ppm) using the following Equation.

$$\%DS = \left\{ \frac{[\text{CH}_3]}{[\text{H}]} \times \frac{5}{6} \right\} \times 100 \quad \dots\dots\dots(4.1)$$

The calculated % DS is in the range of 1-5%. Eventhough the values are low, they are quite reasonable considering that the quaternization occurred at the surface. It should be noted that the calculated values obtained from NMR data are %DS of the whole film. Therefore, they should presumably be lower than the actual %DS in the surface region.

Table 4.5 Degree of methylation of quaternized *N*-alkyl chitosan film

Substrate	Integration		%DS
	H-2',3,4,5,6 of chitosan	-CH ₃ of -N ⁺ R(CH ₃) ₂	
DME film	100	5.8	5
DMP film	100	2.2	2
DMBu film	100	2.0	2
DMBz film	100	0.8	1

ATR-FTIR spectroscopy was also used to confirm the success of quaternization of *N*-alkyl chitosan by MeI. As shown in Figure 4.9, the intensity of the characteristic N-H bending peak of chitosan at 1590 cm⁻¹ correspondingly decreased after the reaction. The peaks in the range of 1480-1440 cm⁻¹ observed on the spectra are the characteristic peaks of C-N stretching and C-H deformation of CH₂(s). The results from the ATR-FTIR analysis also demonstrate that the reaction has proceeded to a depth of at least 1-2 μm (estimated depth of ATR-FTIR sensitivity).

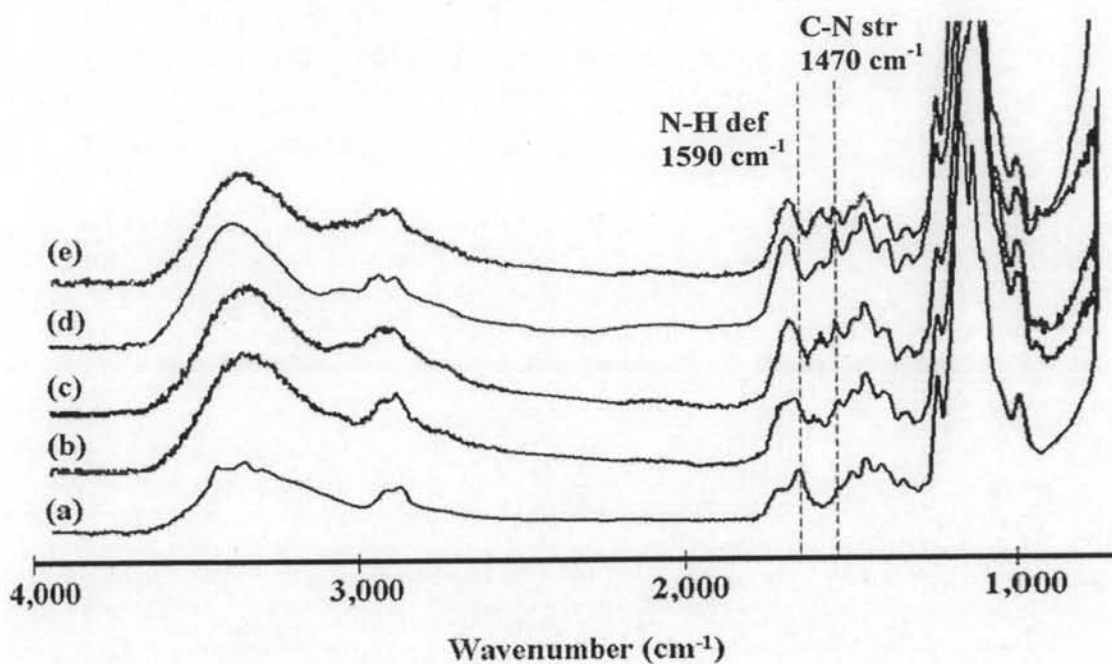
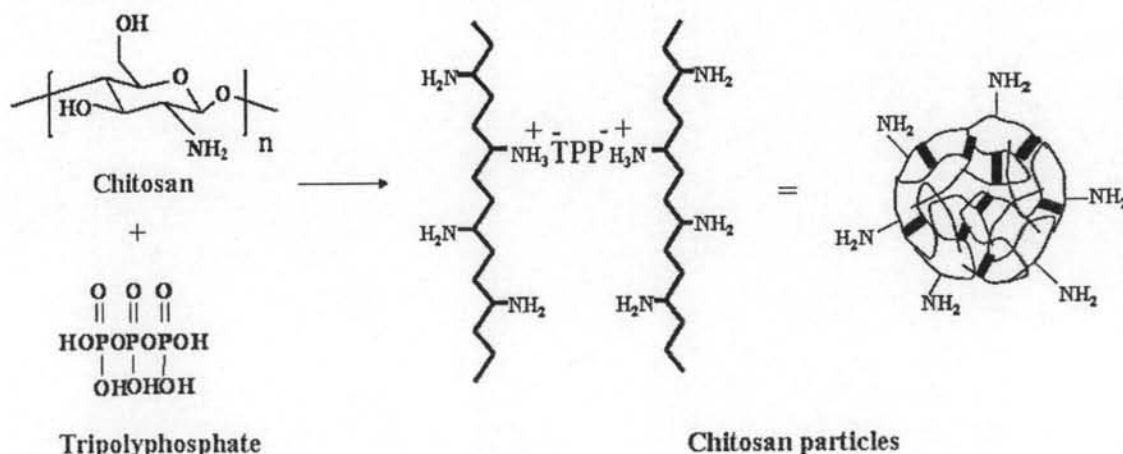


Figure 4.9 ATR-FTIR spectra of (a) unmodified chitosan film, (b) DME film, (c) DMP film, (d) DMBu film and (e) DMBz film

4.4 Preparation of Chitosan Particles

The preparation of chitosan particles is based on an ionic gelation between positively charged chitosan and negatively charged triphosphate at room temperature shown in Scheme 4.2. The chitosan particles prepared in the experiment appear as white fine powder which are insoluble in water, dilute acidic and alkali solution.



Scheme 4.2 Preparation of chitosan particles by ionic gelation between chitosan and triphosphate (TPP)

FT-IR analysis of chitosan and chitosan particles were performed to characterize the chemical structure of particles. As shown in Figure 4.10, the appearance of characteristic peak at 1217 cm^{-1} assigned to P=O groups of TPP and the shifting of the N-H bending signal from 1590 cm^{-1} for chitosan to 1550 cm^{-1} for chitosan particles implied that the ammonium groups are crosslinked with tripolyphosphate molecules.

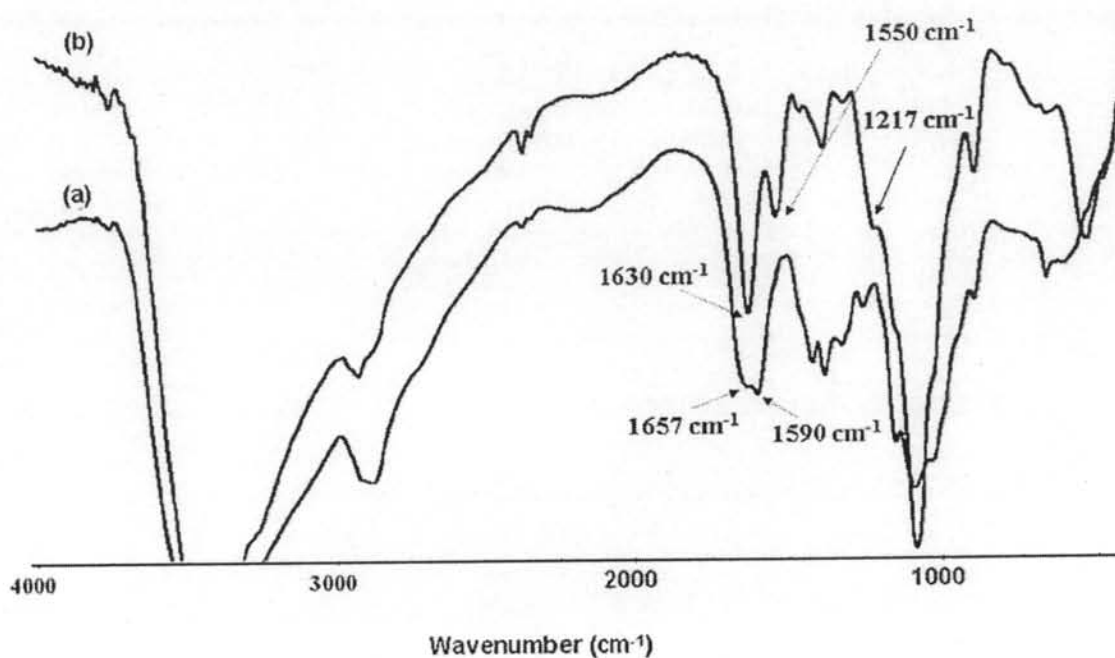


Figure 4.10 FT-IR spectra of (a) chitosan and (b) chitosan particles

4.5 Charge Characteristic of Quaternized *N*-alkyl Chitosan Particles

The presence of quaternary ammonium groups of the quaternized *N*-alkyl chitosan particles prepared by the optimized conditions previously identified was verified by zeta potential measurements. The data are shown in Table 4.6. Obviously, DEM particles are the only samples that exhibit positive charges in the first series of quaternized *N*-alkyl chitosan. The fact that the zeta potential of DBuM particles is negative implies that the quaternization of *N*-methyl chitosan by BuI is somewhat limited. This may be explained by the same reason previously described for OcI. All samples in the second series possess higher zeta potential values in comparison with chitosan particles. In particular, DMBz particles show the highest zeta potential. In order to determine whether we can tailor the charge characteristic of the quaternized

N-alkyl chitosan particles, the preparation of DMBz particles from *N*-benzyl chitosan particles using varied concentration of MeI concentration was investigated. The results from Table 4.7 clearly indicate that the zeta potential increases as a function of MeI concentration.

Table 4.6 Zeta potential of quaternized *N*-alkyl chitosan particles

Substrate	Zeta potential (mV)
Chitosan particles	+13.11
<i>N,N</i> -diethyl- <i>N</i> -methyl chitosan (DEM) particles	+38.00
<i>N,N</i> -dibutyl- <i>N</i> -methyl chitosan (DBuM) particles	-20.00
<i>N,N</i> -dioctyl- <i>N</i> -methyl chitosan (DOcM) particles	n/a
<i>N</i> -ethyl- <i>N,N</i> -dimethyl chitosan (DME) particles	+32.33
<i>N</i> -propyl- <i>N,N</i> -dimethyl chitosan (DMP) particles	+33.51
<i>N</i> -butyl- <i>N,N</i> -dimethyl chitosan (DMBu) particles	+34.93
<i>N</i> -benzyl- <i>N,N</i> -dimethyl chitosan (DMBz) particles	+58.60

Table 4.7 Zeta potential of DMBz particles prepared from *N*-benzyl chitosan particles using varied concentration of MeI

MeI (M)	Zeta potential (mV)
0.4	+13.63
0.6	+34.52
0.8	+45.46
1.2	+49.83
1.6	+62.03
2.0	+58.60

4.6 Antibacterial Activity of Quaternized *N*-alkyl Chitosan Films

The exact mechanism of interaction between chitosan, its derivatives and the microorganism is still unknown, but different mechanisms have been proposed in the explanation of antimicrobial activity. It is believed that the polycationic nature of chitosan initiates the binding with the cell membrane by means of electrostatic attraction with the negatively charged microbial cell membrane. In this study, the antibacterial activities of quaternized *N*-alkyl chitosan films were tested against gram-positive bacteria, *S. aureus* and gram-negative bacteria, *E. coli* using 2 methods: Shake flask method and Plate counting method.

4.6.1 Shake Flask Method

The shake flask method was used as the first method to evaluate the antibacterial activity of the second series of quaternized *N*-alkyl chitosan films. The number of bacteria was determined from the OD₆₀₀ value of the suspension after incubation in the presence of quaternized *N*-alkyl chitosan film which was prepared under the optimized condition. The higher the OD₆₀₀ value, the greater the number of bacteria is. According to Table 4.8, it is obvious that the antibacterial activity of all quaternized *N*-alkyl chitosan films against both *S. aureus* and *E. coli* are superior to the chitosan film. As expected, the chitosan film did not show any antibacterial activity under the testing condition. Since the working pH was in the neutral region, most amino groups of chitosan should be in the form of amino groups (-NH₂), not ammonium groups (-NH₃⁺). We postulate that the highest zeta potential of DMBz accounts for its most effective antibacterial activity in the series. Taking into consideration that DME, DMP and DMBu have similar zeta potential, it seems that the larger the alkyl substituent coming from aldehyde, the greater the antibacterial activity. However, the difference of the OD₆₀₀ between each sample is not significant enough to draw any conclusion at this point.

Table 4.8 Optical density (OD₆₀₀) of *S. aureus* and *E. coli* solution in the presence of different quaternized *N*-alkyl chitosan films

Sample	Water contact angle (°)	Zeta potential (mV)	OD ₆₀₀ (<i>S.aureus</i>)	OD ₆₀₀ (<i>E. coli</i>)
Control ^a	-	-	2.2	1.8
Chitosan film	79.8	+13.11	2.2	1.8
DME film, R=ethyl	71.7	+32.33	1.5	1.5
DMP film, R=propyl	83.6	+33.51	1.4	1.4
DMBu film, R=butyl	84.6	+34.93	1.1	1.2
DMBz film, R=benzyl	75.4	+58.60	0.9	1.2

^a Control is a bacterial solution in the absence of film substrate

Nonetheless, it is still rather difficult to compare the strength of antibacterial activities between each sample in the series because each sample has different extent of quaternization. To determine such a parameter, we desired to investigate the effect of the extent of quaternization on the antibacterial activity of DMBz against *S. aureus*. The extent of quaternization was varied as a function of the concentration of MeI used for quaternization of *N*-benzyl chitosan films (See Table 4.7 for zeta potential). The results from Table 4.9 suggest that the degree of quaternization which should be directly correlated with the zeta potential value truly influences the antibacterial activity. The higher the zeta potential, the lower the OD₆₀₀ and the better the antibacterial activity becomes. It should be noted that the water contact angle became smaller as the extent of quaternization reached a certain value. This implies that the surface charge has a stronger impact on the antibacterial activity than the hydrophobicity/hydrophilicity.

Table 4.9 Optical density (OD₆₀₀) of *S. aureus* in solution in the presence of DMBz films having different degrees of quaternization (varied as a function of MeI)

Sample	Water contact angle (°)	Zeta potential (mV)	OD ₆₀₀ (<i>S. aureus</i>)
Control	-	-	2.46
Chitosan film	79.8	+13.11	2.40
DMBz film, 0.4 M MeI	86.0	+13.63	2.13
DMBz film, 0.8 M MeI	95.4	+45.46	2.20
DMBz film, 1.2 M MeI	95.2	+49.83	2.08
DMBz film, 1.6 M MeI	77.4	+62.03	1.43
DMBz film, 2.0 M MeI	75.4	+58.60	1.40

The bacteria concentration in the suspension can be calculated from the calibration curve shown in Figure 4.11. The straight lines were obtained for both cell suspensions, but the slopes of the lines for the two species were different. This is thought to be due to shape, size distribution and density distribution differences in the cell aggregates.

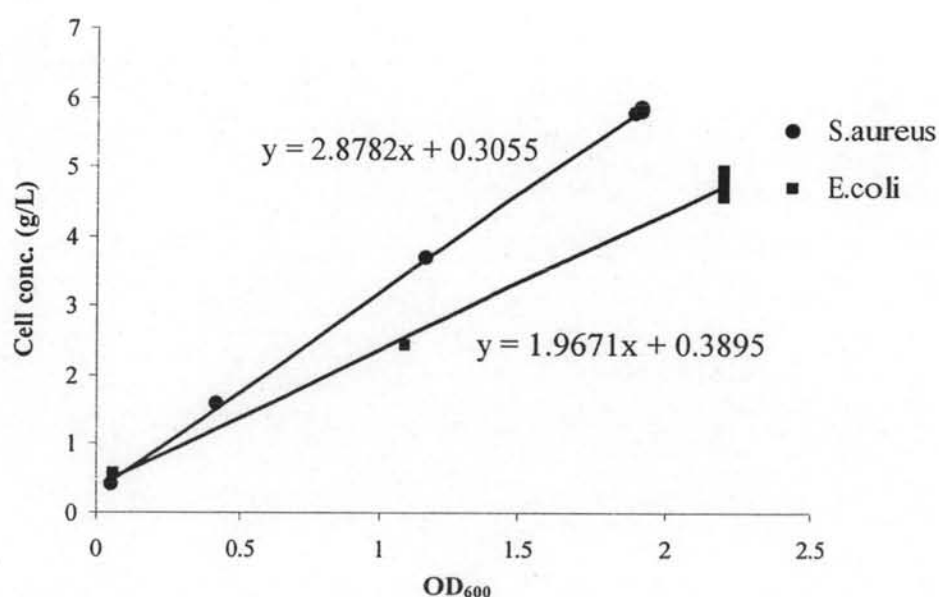


Figure 4.11 Relationship between OD₆₀₀ and cell concentration (g/L) of *S. aureus* and *E. coli* suspensions

Based on the OD₆₀₀ data in Tables 4.8 and 4.9, the bacteria concentration can be estimated. The data are displayed in Figures 4.12-4.13.

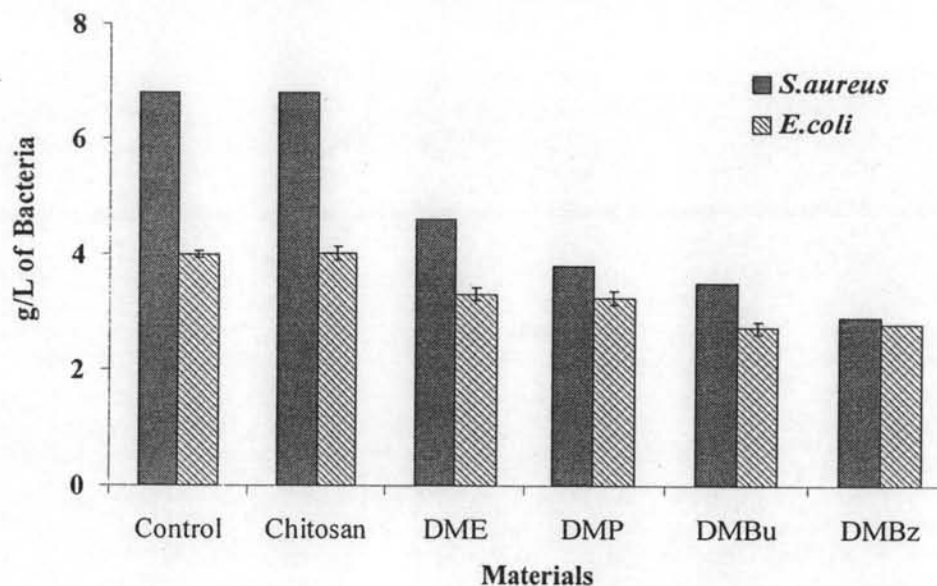


Figure 4.12 Cell concentrations (g/L) of *S. aureus* and *E. coli* in the presence of different quaternized *N*-alkyl chitosan films

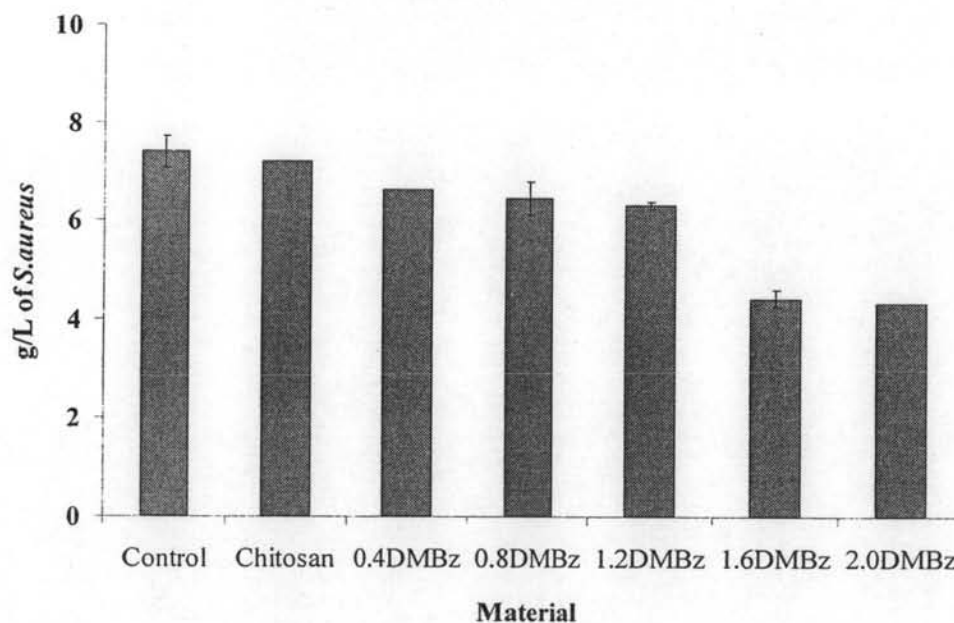


Figure 4.13 Cell concentrations (g/L) of *S. aureus* in the presence of DMBz films having different degrees of quaternization (varied as a function of MeI)

According to the SEM images shown in Figure 4.14, there are fewer *S. aureus* cells adhered on the surface of DMBu film as opposed to the surface of chitosan film suggesting that the DMBu film can inhibit the growth of *S. aureus*. That does not seem to be the case for *E. coli*. Even though there are a greater number of *E. coli* in the solution containing chitosan film than that containing DMBu film (see OD₆₀₀ in Table 4.8), none of them adhered on the surface of chitosan film. It is known that the outer membrane gram negative bacteria (*E. coli*) is composed by phospholipids and lipopolysaccharides of which the lipid portion of faces the external environment. Then, it is thus possible that the greater hydrophobicity of DMBu film than chitosan may be the reason why *E. coli* (see Table 4.8 for contact angle data) can adhere more on than chitosan. Although quite a few are present on the surface of DMBu film, their surface is severely damaged. This may be caused by the blocking of the channels at the surface of *E. coli* called porins by the DMBu films. The molecules ions, sugar and amino acids which are essential to the metabolism of the bacteria cannot transport across the outer membrane. So the bacteria cannot survive. It is not yet clear whether the number of adhered bacteria has any correlation with the viability of the bacteria. For this reason, the determination of antibacterial activities using a plate counting method which is a more sensitive technique towards the bacteria viability was conducted.

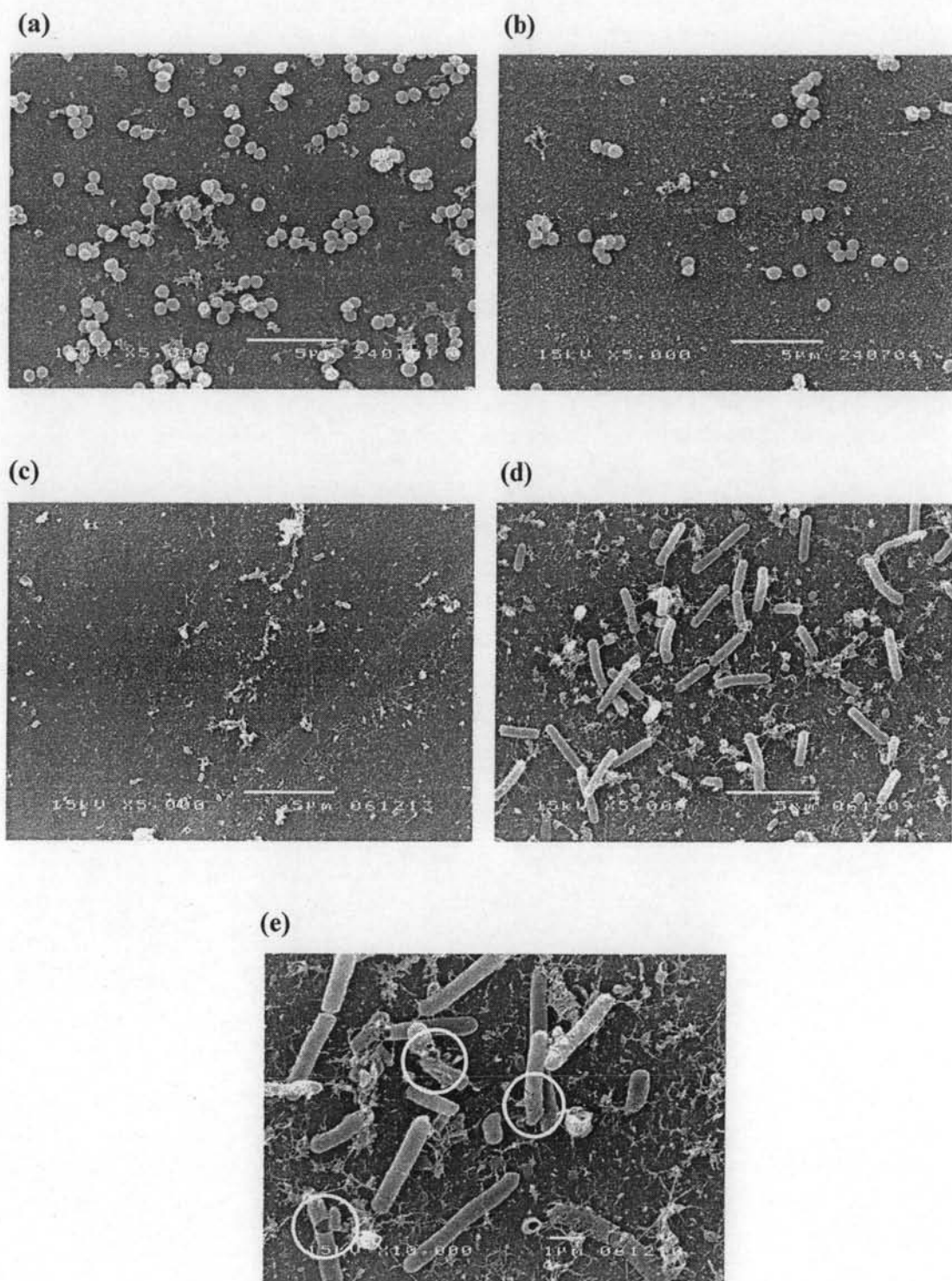


Figure 4.14 Scanning electron micrographs of (a) chitosan film after being exposed to *S. aureus*, (b) DMBu film after being exposed to *S. aureus*, (c) chitosan film after being exposed to *E. coli*, (d) DMBu film after being exposed to *E. coli* ($\times 5,000$) and (e) DMBu film after being exposed to *E. coli* ($\times 10,000$)

4.6.2 Plate Counting Method

Unlike the shake flask method, the plate counting method is a more sensitive technique towards the bacteria viability. The bacterial solution after exposing to the quaternized *N*-alkyl chitosan film was pour-plated onto the triplicate solid agar using the spread plate method. After incubating at 37°C for 18 h, a number of viable bacteria were then counted. The results after multiplication with the dilution factor were expressed as mean colony forming units per volume (CFU/mL).

In order to determine the effect of alkyl substituent on the antibacterial activity against *S. aureus* and *E. coli* of the second series of quaternized *N*-alkyl chitosan films, DME, DMP, DMBu and DMBz films having similar zeta potential (~ 30 mV) were selected for the investigation. It is assumed that the zeta potential can reflect the degree of quaternization to some extent. The OD₆₀₀ values of both bacteria after exposure to the quaternized *N*-alkyl chitosan films shown in Figure 4.14 suggest that DME and DMBu exhibit higher antibacterial activities than DMP and DMBz against both bacteria. The OD₆₀₀ is more statistically different from one another as compared with the data previously seen from the shake flask method. This may be due to that the greater ratio between the surface area of the quaternized *N*-alkyl chitosan film and the bacterial concentration being used for the spread plate method. Nonetheless, we cannot find any correlation between the size of alkyl group and antibacterial activity.

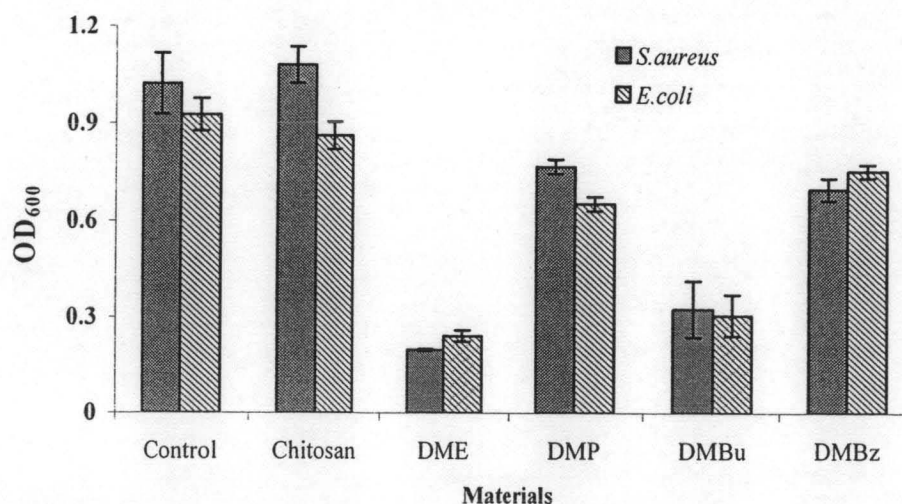


Figure 4.15 Optical densities (OD₆₀₀) of *S. aureus* and *E. coli* solution in the presence of different quaternized *N*-alkyl chitosan films having similar zeta potential

The number of viable counts and antibacterial ratio of the quaternized *N*-alkyl chitosan films is displayed in Table 4.10 followed the same trend of the OD₆₀₀ values shown in Figure 4.14. It seems that all quaternized *N*-alkyl chitosan films are more vital to *E. coli* than *S. aureus*. It is suspected that the presence of alkyl group of the quaternized *N*-alkyl chitosan film may promote the hydrophobic interaction with *E. coli*, a gram-negative bacterium, whose cell wall is mainly covered by phospholipids bilayer.

Table 4.10 Viable counts and antibacterial ratio of *S. aureus* and *E. coli* in the presence of different quaternized *N*-alkyl chitosan films having similar zeta potential

Sample	Viable counts (CFU/mL)		Antibacterial ratio (%)	
	<i>S. aureus</i>	<i>E. coli</i>	<i>S. aureus</i>	<i>E. coli</i>
Control	3.14×10^{12}	6.00×10^{12}	0	0
Chitosan film	3.21×10^{12}	5.89×10^{12}	< 0	1.8
DME film, R=ethyl	6.60×10^{11}	3.20×10^{11}	79	95
DMP film, R=propyl	1.09×10^{12}	1.05×10^{12}	65	83
DMBu film, R=butyl	4.80×10^{11}	2.10×10^{11}	85	97
DMBz film, R=benzyl	8.70×10^{11}	9.80×10^{11}	72	84

In order to verify the effect of degree of quaternization on the antibacterial activity, the same set of DMBz films used for the shake flask method (see Table 4.9) were tested against both *E. coli* and *S. aureus* using the plate counting method. The results shown in Figure 4.15 and Table 4.11 are in accord with the data obtained from the shake flask method. The higher the zeta potential, the lower the OD₆₀₀ and the better the antibacterial activity becomes. The highly quaternized DMBz films prepared using 1.6 M and 2.0 MeI are so potent that they can essentially suppress the bacteria growth (100% antibacterial ratio).

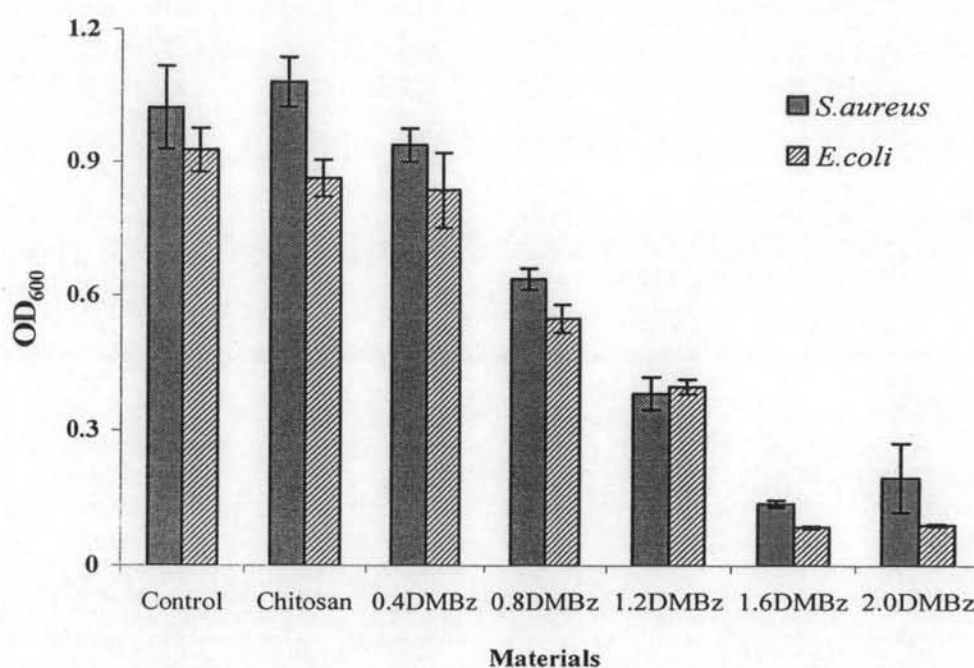


Figure 4.16 Optical densities (OD₆₀₀) of *S. aureus* and *E. coli* in solution in the presence of DMBz films having different degrees of quaternization (varied as a function of MeI)

Table 4.11 Viable cells and antibacterial ratio of *S. aureus* and *E. coli* in solution in the presence of DMBz films having different degrees of quaternization (varied as a function of MeI)

Sample	Viable counts (CFU/ml)		Antibacterial ratio (%)	
	<i>S. aureus</i>	<i>E. coli</i>	<i>S. aureus</i>	<i>E. coli</i>
Control	3.14×10^{12}	6.00×10^{12}	0	0
Chitosan film	3.21×10^{12}	5.89×10^{12}	< 0	1.8
DMBz film, 0.4 M MeI	1.58×10^{12}	4.95×10^{12}	54	18
DMBz film, 0.8 M MeI	8.70×10^{11}	9.40×10^{11}	72	84
DMBz film, 1.2 M MeI	2.90×10^{11}	3.40×10^{11}	91	94
DMBz film, 1.6 M MeI	0	0	100	100
DMBz film, 2.0 M MeI	4.00×10^{10}	3.00×10^{10}	99	100